25049

The positional influence of the helical geometry of the heteroduplex substrate on human RNase H1 catalysis

Walt F. Lima, John B. Rose, Josh G. Nichols, Hongjiang Wu, Michael T. Migawa, Tadeusz K. Wyrzykiewicz, Guillermo Vasquez, Eric E. Swayze and Stanley T. Crooke

Department of Molecular and Structural Biology

Isis Pharmaceuticals

Molecular Pharmacology Fast Forward. Published on October 6, 2006 as DOI: 10.1124/mol.106.025429
This article has not been copyedited and formatted. The final version may differ from this version.

25049

Running title: Effects of substrate structure on human RNase H1 activity

Walt Lima

2292 Faraday Ave.

Carlsbad, CA. 92008

Ph. (760) 603-2387

Fax (760) 931-0209

Email: wlima@isisph.com

Text pages: 36

Figures: 8

References: 17

Abstract: 250 words

Introduction: 739 words

Discussion: 1580

Abbreviations: 2'-methoxyethyl (MOE), antisense oligonucleotides (ASO),

Molecular Pharmacology Fast Forward. Published on October 6, 2006 as DOI: 10.1124/mol.106.025429
This article has not been copyedited and formatted. The final version may differ from this version.

Abstract

In a companion study we showed that chimeric substrates containing 2'-methoxyethyl (MOE) nucleotides inhibited human RNase H1 activity. Here, we prepared chimeric substrates containing a central DNA region with flanking northern biased MOE nucleotides hybridized to complementary RNA. Conformationally biased and flexible modified nucleotides were positioned at the junctions between the DNA and MOE residues of the chimeric substrates to modulate the effects of the MOE residues on human RNase H1 activity. The strong northern biased Locked-nucleic acid modification exacerbated the negative effects of the MOE modifications resulting in slower human RNase H1 cleavage rates. Enhanced cleavage rates were observed for the eastern biased 2'-ara-fluorothymidine and bulge inducing N-methylthymidine modifications positioned at the 5'-DNA/3'-MOE junction as well as the southern biased 2'-methylthiothymidine and conformationally flexible tetrafluoroindole (TFI) modifications positioned at the 5'-MOE/3'-DNA junction. The heterocycle of the ribonucleotide opposing the TFI deoxyribonucleotide had no effect on the human RNase H1 activity whereas nucleotide substitutions adjacent the TFI significantly affected the cleavage rate. Mismatch base-pairs exhibited similar effects on human RNase H1 activity as the TFI modifications. The effects of the TFI modification and mismatch base-pairs on human RNase H1 activity were influenced by the position of the modification relative to the nucleotides interacting with the catalytic site of the enzyme rather than the juxtaposition of the modification to the MOE residues. Finally, these results provide a method for

Molecular Pharmacology Fast Forward. Published on October 6, 2006 as DOI: 10.1124/mol.106.025429
This article has not been copyedited and formatted. The final version may differ from this version.

enhancing the human RNase H1 activity of chimeric antisense oligonucleotides (ASO) as well as the design of more potent ASO drugs.

Molecular Pharmacology Fast Forward. Published on October 6, 2006 as DOI: 10.1124/mol.106.025429
This article has not been copyedited and formatted. The final version may differ from this version.

Human RNase H1 has been shown to play a dominant role in the activity of DNA-like antisense oligonucleotides (Wu, 2004). In several cell lines, the human RNase H1 protein was both overexpressed and reduced using DNA-like antisense oligonucleotides (ASOs) and small interfering RNAs (siRNAs) targeting the mRNA of the enzyme. The effects of these manipulations on the potencies of a number of DNA-like ASOs to several different target RNAs showed that increasing the level and activity of human RNase H1 increased the potency of the ASOs and reducing the level of the enzyme resulted in a commensurate reduction in the potency of the ASOs (Wu, 2004). Moreover, overexpression of human RNase H1 in mouse liver increased the potency of a DNA-like ASO targeting Fas after IV administration.

We have demonstrated that human RNase H1 is comprised of an RNA-binding domain, a spacer region and a catalytic domain (Wu, 2001). Once bound to the heteroduplex substrate, the RNA-binding and the catalytic domains are separated by approximately one helical turn with the RNA binding-domain positioned 3' on the RNA to the catalytic domain (Lima, 2003). The RNA-binding domain is responsible for the strong positional preference for cleavage exhibited by the enzyme and modified nucleotides effecting the interaction between the RNA-binding domain and the substrate produced a shift in the cleavage pattern, i.e., ablation of the 5'-most cleavage site (Lima, 2003). The catalytic domain, on the other hand, is highly sensitive to modifications that alter the geometry of the minor groove surrounding the cleavage site (Lima, 2004). To be cleaved by

Molecular Pharmacology Fast Forward. Published on October 6, 2006 as DOI: 10.1124/mol.106.025429
This article has not been copyedited and formatted. The final version may differ from this version.

human RNase H1, a substrate must display a minor groove of appropriate dimensions unobstructed by 2'-modifications of the deoxyribose. Further, the intra and interphosphate distances of the heteroduplex substrate are crucial as is the flexibility of the backbone (Lima, 2004).

Several factors influence the therapeutic utility of ASOs including, but not limited to, the affinity for the target RNA, the terminating mechanism, (e.g., RNase H), pharmacokinetics and toxicological properties (For review see Crooke, 2001). Chimeric ASO configurations designed to take into account these factors have resulted in ASOs with improved potency (For review see Crooke, 2001). These chimeric ASOs consist of a deoxyribonucleotide region to support RNase H activity flanked by modified nucleotides, (e.g., 2'-methoxyethyl (MOE) nucleotides) for enhanced hybridization affinity, increased nuclease resistance and reduced pro-inflammatory effects. MOE nucleotides exhibit a RNA-like C_3-*endo* sugar conformation and an A-form helical conformation when hybridized to RNA. In addition, the proximity of the 2'-methoxyethyl to the phosphate backbone results in further stabilization of the duplex via an extensive hydration network between the 2'-methoxyethyl oxygens and the bridging and non-bridging phosphate oxygens (Teplova, 1999). The conformation induced by the (MOE) nucleotides results in a 0.9 – 1.5°/modification increase in the T_m of the ASO/RNA duplex, enhanced nuclease resistance presumable due to steric hindrance of the nuclease by the 2'-methoxyethyl and elimination half-lives ranging from 14 to 30 days in all species including man (Freier, 1997; Crooke, 2001). Nevertheless,

Molecular Pharmacology Fast Forward. Published on October 6, 2006 as DOI: 10.1124/mol.106.025429
This article has not been copyedited and formatted. The final version may differ from this version.

heteroduplexes containing chimeric ASOs exhibit slower human RNase H1 cleavage rates compared to unmodified substrates (see companion study). Furthermore, any modification of the antisense DNA can have a profound influence on the overall catalytic rate, the site of cleavage as well as the cleavage rates of specific sites. To better understand the mechanisms of the observed reduction in catalytic efficiency of chimeric substrates containing 2'-modified nucleotides and to begin to identify means to mitigate these effects, we introduced modified nucleotides at the MOE/DNA junction of the chimeric ASO to modulate the transmission of conformation of the MOE substitutions into the area of the duplex in which cleavage occurs (Fig. 1). In addition, mismatched base-pairs were introduced at various positions in the chimeric substrate and the initial cleavage rates (V_0) for the modified heteroduplexes were compared with the wild type DNA/RNA heteroduplex.

Molecular Pharmacology Fast Forward. Published on October 6, 2006 as DOI: 10.1124/mol.106.025429
This article has not been copyedited and formatted. The final version may differ from this version.

Materials and Methods

Synthesis of oligonucleotides

The oligoribonucleotides were synthesized using 5'-*O*-silyl-2'-*O*-bis(2-acetoxyethoxy)methyl ribonucleoside phosphoramidites and procedures described elsewhere (Scaringe, 1998). The 5'-*O*-(4,4'-dimethoxytrityl)-2'-deoxy-2'-fluoro-arabino-thymidine-3'-[(2-cyanoethyl)-*N,N*-diisopropyl]phosphoramidite and 5'-*O*-(4,4'-dimethoxy-trityl)-N-Methyl-5-methyluridine-3'-[(2-cyanoethyl)-*N,N*-diisopropyl]phosphoramidite was purchased from RI Chemicals (Orange, CA) or other commercial sources. 5'-*O*-(4,4'-Dimethoxy-trityl)-tetra-fluoro-indole-3'-[(2-cyanoethyl)-*N,N*-diisopropyl]-phosphoramidite and 5'-*O*-(4,4'-dimethoxytrityl)-2'-*S*-methyl-2'-thio-5-methyluridine-3'-[(2-cyanoethyl)-*N,N*-diisopropyl]phosphoramidite were synthesized as described previously (Lai and Kool, 2004; Fraser, 1993). Standard 2'-deodxynucleoside phosphoramidites and solid supports were obtained from Glen Research and used for incorporation of A, T, G, and C residues as 0.1 M solutions in anhydrous. All oligonucleotides were synthesized on functionalized Controlled-Pore Glass on an automated solid-phase DNA synthesizer with the final dimethoxytrityl group retained at 5'-end. For incorporation of modified amidites (LNA, TFI, 2'-S-Me-T, N-Me-T), their 0.2 M solutions in acetonitrile (6 eq/coupling) of phosphoramidite solutions were delivered in two portions, each followed by a 6-min coupling wait time. All other steps in the protocol supplied by the manufacturer were used without modification.

Molecular Pharmacology Fast Forward. Published on October 6, 2006 as DOI: 10.1124/mol.106.025429
This article has not been copyedited and formatted. The final version may differ from this version.

Oxidation of the internucleotide phosphite to the phosphate was carried out using a 0.1 M solution of iodine in 20:1 (v/v) pyridine/water with a 10-min oxidation wait time. The average coupling efficiencies were >97%. To deprotect oligonucleotides containing 2'-deoxy-2'-fluorothymidine and 2'-deoxy-2'-fluoroarabinofuranosylthymine, the solid supports bearing the oligonucleotides were suspended in aqueous ammonia (28–30 weight %)/ethanol (3:1; 3 ml for 2-µmol scale synthesis) and heated at 55 °C for 6 h. For all other modified oligonucleotides after completion of the synthesis, the solid supports bearing the oligonucleotides were suspended in aqueous ammonium hydroxide (28–30 weight %; 1 ml / 1-µmol) and kept at room temperature for 2 h. The solid support was filtered, and the filtrate was heated at 55 °C for 6 h to complete the removal of all protecting groups. Crude oligonucleotides were purified on a Waters HPLC C_4 7.8 x 300-mm column (buffer A = 100 mM ammonium acetate (pH 6.5–7); buffer B = acetonitrile; 5–60% of buffer B in 55 min) at a flow rate of 2.5 ml/min ($A_{260\ nm}$). Detritylation was achieved by adjusting the pH of the solution to 3.8 with acetic acid and by keeping at room temperature until complete removal of the trityl group, as monitored by HPLC analysis. The oligonucleotides were then desalted by HPLC to yield modified oligonucleotides in 30–40% isolated yield calculated based on the loading of the 3'-base onto the solid support. The oligonucleotides were characterized by electrospray mass spectroscopy, and their purity was assessed by HPLC and capillary gel electrophoresis. The purity of the oligonucleotides was >95%.

Molecular Pharmacology Fast Forward. Published on October 6, 2006 as DOI: 10.1124/mol.106.025429
This article has not been copyedited and formatted. The final version may differ from this version.

Preparation of the heteroduplex substrates

Human RNase H1 containing an N-terminal His-tag was expressed and purified as previously described (Lima, 2001). The RNA substrate was 5'-end-labeled and purified as previously described (Lima, 2001; Sambrook, 1989). The specific activity of the labeled oligonucleotide is approximately 3000 to 8000 cpm/fmol. The heteroduplex substrate was prepared in 100 µL containing unlabeled oligoribonucleotide ranging from 100 to 1000 nM, 10^5 cpm of ^{32}P labeled oligoribonucleotide, two-fold excess complementary oligodeoxyribonucleotide and hybridization buffer [20 mM tris, pH 7.5, 20 mM KCl]. Reactions were heated at 90° C for 5 min, cooled to 37° C and 60 U of Prime RNase Inhibitor (5 Prime $\rightarrow$ 3 Prime, CO) and $MgCl_2$ at a final concentration of 1 mM were added. Hybridization reactions were incubated 2 - 16 h at 37° C and 1 mM tris(2-carboxyethyl)phosphate (TCEP) was added.

Multiple-turnover kinetics

The human RNase H1 proteins were incubated with dilution buffer (50 mM tris, 50 mM NaCl, 100 µM TCEP, pH 7.5) for 1 h at 24° C. The heteroduplex substrate was prepared in triplicate and each preparation was digested with 0.4 ng of enzyme at 37° C. A 10 µl aliquot of the cleavage reaction was removed at time points ranging from 2 - 120 min and quenched by adding 5 µL of stop solution (8 M urea and 120 mM EDTA). The aliquots were heated at 90° C for 2 min, resolved in a 12% denaturing polyacrylamide gel and the substrate and product

Molecular Pharmacology Fast Forward. Published on October 6, 2006 as DOI: 10.1124/mol.106.025429
This article has not been copyedited and formatted. The final version may differ from this version.

bands were quantitated on a Molecular Dynamics PhosphorImager. The concentration of the converted product was plotted as a function of time. The initial cleavage rate (V_0) was obtained from the slope (mole RNA cleaved/min) of the best-fit line for the linear portion of the plot, which comprises, in general < 10% of the total reaction and data from at least five time points.

Molecular Pharmacology Fast Forward. Published on October 6, 2006 as DOI: 10.1124/mol.106.025429
This article has not been copyedited and formatted. The final version may differ from this version.

Results

Modified nucleotides were introduced at the MOE-DNA junctions of chimeric oligonucleotides to modulate the conformational transmission of the flanking MOE/RNA regions into the central DNA/RNA region (Fig. 2). The conformationally biased modified nucleotides included the RNA-like northern $C_{3'}$-*endo* Locked nucleic acids (LNA), the DNA-like southern $C_{2'}$-*endo* 2'-methylthiothymidine (2'-S-Me-T) and eastern $O_{4'}$-*endo* 2'-ara-fluorothymidine (2'-ara-F-T) (Fig. 1A). The modified nucleotides predicted to introduce comformational flexibility at the MOE-DNA junctions included the 2'-methoxyethyl-N-methylthymidine (N-Me-T) and tetrafluoroindole (TFI) (Fig, 1B). The conformationally flexible modifications contain hydrophobic heterocycle bases predicted to Π-stack with adjacent nucleotides, but not form hydrogen bonds with the opposing RNA. The modified ASOs were annealed to complementary RNA and the heteroduplexes digested with human RNase H1 under multiple-turnover conditions as described in Materials and Methods.

The MOE residues negatively affected human RNase H1 activity. For example, the cleavage rates for the chimeric heteroduplexes containing flanking MOE residues (5-10-5, 4-11-5 and 5-11-4) were approximately 3-fold slower than the cleavage rate observed for the heteroduplex without MOE residues (0-10-0) (Fig.2). Replacing a single MOE residue with a deoxyribonucleotide at the

Molecular Pharmacology Fast Forward. Published on October 6, 2006 as DOI: 10.1124/mol.106.025429
This article has not been copyedited and formatted. The final version may differ from this version.

junctions (positions 5 and 16) had no effect as the 4-11-5 and 5-11-4 substrates exhibited cleavage rates similar to the 5-10-5 substrate (Fig.2).

The human RNase H1 cleavage rates for the heteroduplexes containing the junction modifications at the 5'-MOE/3'-DNA junction (position 5) are shown in figure 2. The northern biased LNA at position 5 resulted in a 35% slower cleavage rate compared to the parent 5-10-5 substrate. In contrast, the southern biased 2'- S-Me-T modification enhanced the cleavage rate. The eastern biased 2'-ara-F-T modification had no effect on the human RNase H1 activity when substituted at position 5, i.e., comparable cleavage rates were observed for the 2'-ara-F-T heteroduplex and the 5-10-5 substrate. The N-Me-T modification, which does not form hydrogen bonds with the opposing ribonucleotide and is predicted to create a bulge in the heteroduplex also had no effect on human RNase H1 activity compared with the 5-10-5 substrate. The TFI deoxyribonucleotide, on the other hand, enhanced the human RNase H1 cleavage rate when substituted at position 5 (Fig. 2). This modification also does not form a hydrogen bond with the opposing ribonucleotide but is predicted to Π-stack between the adjacent nucleotides.

Very different results were observed for the same nucleotide modifications positioned at the 5'-DNA/3'-MOE junction (position 16). Again, the northern biased LNA substitution resulted in slower cleavage rates (Fig. 2). However, the bulge inducing N-Me-T modification as well as the eastern biased 2'-ara-F-T at

Molecular Pharmacology Fast Forward. Published on October 6, 2006 as DOI: 10.1124/mol.106.025429
This article has not been copyedited and formatted. The final version may differ from this version.

position 16 increased the cleavage rate compared with the 5-10-5 substrate and yet both the TFI and 2'-S-Me-T modifications, which resulted in faster cleavage rates when substituted at position 5, had no effect on the cleavage rate at position 16 (Fig. 2). Finally, the overall cleavage rates as well as the cleavage sites for the 5-10-5, 4-11-5 and 5-11-4 heteroduplexes were equivalent, demonstrating that simply increasing the length of the DNA portion of the heteroduplex with a modified deoxyribonucleotide substitution at the junction can not account for the effects induced by the junction modifications (Fig. 2).

The junction modifications affected the cleavage patterns as well as the cleavage rates for the sites nearest the junction modification (Fig. 2 and 3). For example, both the 0-10-0 and 5-10-5 heteroduplexes exhibited two cleavage sites 10 and 12 ribonucleotides from the 5'-terminus of the oligoribonucleotide, although the cleavage rates for these sites were significantly slower for the 5-10-5 substrate (Fig. 2 and 3A). Similar cleavage sites were observed for the 4-11-5 and 5-11-4 substrates but again, the cleavage rates at these sites were significantly slower compared with the 0-10-0 substrate (Fig. 2 and 3). The slower cleavage rates observed for the LNA substitutions were reflected in the cleavage patterns. Specifically, the LNA substitution at position 5 ablated the cleavage activity nearest the modification (ribonucleotide 12) and slowed the cleavage rate at ribonucleotide 10 resulting in a 35% slower overall cleavage rate. The LNA substitution at position 16 reduced the rates of cleavage at both sites, but did not ablate cleavage at ribonucleotide 10 (Fig. 2). Conversely, the 2'-S-Me-T

Molecular Pharmacology Fast Forward. Published on October 6, 2006 as DOI: 10.1124/mol.106.025429
This article has not been copyedited and formatted. The final version may differ from this version.

substitution at position 5 enhanced the cleavage activity of the nearest cleavage site at ribonucleotide 12. Enhanced cleavage rates were also observed at ribonucleotide 10 for the 2'-ara-F-T and N-Me-T at position 16 (Fig. 2). Finally, the greatest enhancement in RNase H1 activity was observed for TFI modification at position 5 and this substitution produced two new human RNase H1 cleavage sites at ribonucleotides 11 and 13 (Fig. 2 and 3B).

Given that the TFI deoxyribonucleotide showed the greatest improvement in activity compared with the 5-10-5 substrate, the structure induced by this modification was evaluated in more detail. The TFI modification is isosteric with purine deoxyribonucleotides. Therefore the adenosine ribonucleotide opposing the TFI at position 5 creates a purine-purine base-pair whereas the uridine ribonucleotide opposing the TFI at position 15 creates pyrimidine-purine base-pair. The adenosine ribonucleotide opposing the TFI deoxyribonucleotide at position 5 was substituted with uridine and the uridine ribonucleotide opposing the TFI deoxyribonucleotide at position 15 was substituted with adenosine (Fig. 4). Neither, the uridine substitution opposing the TFI at position 5 (U/TFI (5)) and the adenosine substitution opposing the TFI at position at position 15 with (A/TFI (15)) had an effect on the cleavage activity (Fig. 4). Interestingly, shifting the TFI deoxyribonucleotide from an opposing adenosine ribonucleotide (position 5) to an opposing uridine (position 6) resulted in an approximate 2-fold slower cleavage rate (Fig.

Molecular Pharmacology Fast Forward. Published on October 6, 2006 as DOI: 10.1124/mol.106.025429
This article has not been copyedited and formatted. The final version may differ from this version.

5). In contrast, shifting the TFI deoxyribonucleotide from an opposing adenosine ribonucleotide (position 16) to an opposing uridine (position 15) resulted in an approximately 2-fold faster cleavage rate (Fig. 5). Together, these data suggest that the effects of the TFI deoxyribonucleotide on the human RNase H1 activity appear to depend on the position of the modification within the heteroduplex and not on the heterocycle base of the opposing ribonucleotide.

To better understand how the position of the TFI deoxyribonucleotide within the chimeric heteroduplex influences the affects of the modification on human RNase H1 activity, we substituted the TFI deoxyribonucleotide at various positions within the ASO. Specifically, the TFI deoxyribonucleotide was positioned one to five base-pairs downstream of the nearest cleavage site at ribonucleotide 12 and two to six base-pairs upstream of the nearest cleavage site at ribonucleotide 10 (Fig. 5). The TFI substitutions positioned between the MOE residues and furthest from the human RNase H1 cleavage sites, (e.g., TFI at positions 4 and 17) appeared to have no effect on the enzyme activity compared to the 5-10-5 substrate (Fig. 5). These TFI substitutions were positioned five to six base-pairs from the nearest human RNase H1 cleavage sites. Further, no effect on enzyme activity was observed for the TFI substitutions at positions 6 and 16, which were positioned at the MOE-DNA junctions and, respectively, 4 and 5 base-pairs from the nearest cleavage sites. Conversely, the TFI substitutions at positions 5 and 15 which were also positioned at the MOE-DNA junction and in this case, three base-pairs from the nearest cleavage sites, resulted in an approximate 2-fold

Molecular Pharmacology Fast Forward. Published on October 6, 2006 as DOI: 10.1124/mol.106.025429
This article has not been copyedited and formatted. The final version may differ from this version.

improvement in human RNase H1 activity (Fig. 5). A similar improvement in cleavage activity was observed for the TFI substitution at position 14 which was situated two base-pairs upstream of the nearest cleavage site and one base-pair removed from the MOE-DNA junction. Slower cleavage rates were observed for TFI substitutions at positions 7 and 8 which were two and one base-pairs downstream from the nearest cleavage site and, respectively, one and two base-pairs away from the MOE-DNA junction. Finally, the TFI substitution positioned 2 base-pairs downstream of the nearest cleavage site (position 13) had no effect on human RNase H1 activity (Fig. 5). Clearly, the proximity of the modification to the human RNase H1 cleavage sites had a greater influence on enzyme activity than the juxtaposition of the TFI modification to the MOE residues.

The TFI deoxyribonucleotides are predicted to form stable Π-stacking interactions with the heterocycle bases of the adjacent nucleotides. To evaluate the contribution of the adjacent nucleotides on the effects induced by the TFI deoxyribonucleotides, mismatch base-pairs were introduced adjacent to the TFI deoxyribonucleotides (Fig. 6). Mismatch base-pairs adjacent to the TFI deoxyribonucleotides appeared to negate the influence of the TFI deoxyribonucleotides on human RNase H1 activity. For example, the TFI substitutions at positions 5, 14 and 15 enhanced the cleavage rate approximately 2-fold compared with the 5-10-5 substrate. The introduction of mismatch base-pairs adjacent to the these substitutions reduced the cleavage rate approximately 2-fold, resulting in cleavage rates comparable to the 5-10-5 substrate

Molecular Pharmacology Fast Forward. Published on October 6, 2006 as DOI: 10.1124/mol.106.025429
This article has not been copyedited and formatted. The final version may differ from this version.

heteroduplex without the TFI substitution (Fig. 6). Conversely, the slower cleavage rate observed for the TFI substitution at position 7 was negated with the mismatch base-pair at position 6 resulting in a cleavage rate comparable to the 5-10-5 substrate. Finally, while the TFI substitution at position 8 had no effect on the cleavage rate, the introduction either a C/C or C/A mismatch at position 7 caused a reduction in the cleavage rate (Fig. 6).

To determine whether mismatch base-pairs exhibit similar effects on human RNase H1 to those observed for the TFI deoxyribonucleotides, mismatches were introduced at the positions of the TFI substitutions (Fig. 7). Again, the affects of the mismatch base-pairs on human RNase H1 activity appeared to be influenced by the position of the mismatch relative to the cleavage sites and in most cases, similar effects on cleavage activity were observed for both the TFI and mismatch base-pair substitutions. For example, similar to the TFI substitution at position 4, a G/A or G/G mismatch at this position had no effect on the cleavage activity (Fig. 7A). Similar cleavage activities were also observed for the U/G mismatch and the TFI substitution at position 6 as well as the C/A mismatch and TFI substitution at position 7 (Fig. 7A). Both the C/C and C/T mismatches at position 14 produced a similar 2-fold increase in the cleavage rate as the TFI deoxyribonucleotide at this position (Fig. 7B). Interestingly, the A/A mismatches at positions 5, 15 and 16 resulted in slower cleavage rates compared to the TFI substitutions at these positions (Fig. 7).

Molecular Pharmacology Fast Forward. Published on October 6, 2006 as DOI: 10.1124/mol.106.025429
This article has not been copyedited and formatted. The final version may differ from this version.

Discussion

The heteroduplexes containing flanking northern biased MOE residues (5-10-5, 4-11-5 and 5-11-4) were cleaved significantly slower than the heteroduplexes without the MOE substitutions (0-10-0) (Fig. 2). In addition, slower cleavage rates were observed for the cleavage sites closest to the MOE substitutions. Given that A-form duplexes do not support human RNase H1 activity, the solution structures of chimeric heteroduplexes containing RNA-like 2'-modified nucleotides are consistent with these observations (Lima, 2004). The solution structures showed the northern C3-*endo* biased 2'-modified residues of the chimeric heteroduplexes as well as the adjacent deoxyribonucleotides produced an A-form helical geometry when hybridized to the complementary RNA (Nishizaki, 1997). Only the central deoxyribonucleotides exhibited an O4-*endo* sugar pucker and the characteristic H-form helical geometry of RNA/DNA heteroduplexes (Nishizaki, 1997). The effect of the northern biased modifications on human RNase H1 activity was further supported by the locked nucleic acid (LNA) which are locked in the northern C3-*endo* pucker and resulted in slower cleavage rates when positioned at the DNA/MOE junctions (Figures 2 and 8B) (Bondensgaard, 2000).

The positional effects of the junction modifications, (e.g., position 5 versus position 16) are likely due to the binding directionality of the enzyme on the substrate (Fig. 2). Specifically, human RNase H1 is predicted to bind the heteroduplex substrate with the RNA-binding domain of the enzyme positioned

Molecular Pharmacology Fast Forward. Published on October 6, 2006 as DOI: 10.1124/mol.106.025429
This article has not been copyedited and formatted. The final version may differ from this version.

adjacent to the 5'-DNA/3'-MOE junction (position 16) and the catalytic domain positioned adjacent to the 5'-MOE/3'-DNA junction (position 5) (Fig. 8C) (Lima, 2003). The RNA-binding domain of human RNase H1 is responsible for proper positioning of the enzyme on the substrate and modifications that disrupt this interaction have been shown to produce a shift in the cleavage pattern (Lima, 2003). Given that no shift in the cleavage pattern was observed for the heteroduplexes containing junction modifications closest the RNA-binding domain (position 16) these results suggest that the junction modifications are affecting changes in the positioning of the enzyme on the substrate (Fig. 2). Instead, the positional effects of the junction modifications are consistent with previous observations in which modified nucleotide substitutions were shown to affect the interactions between the substrate and the catalytic domain of the enzyme (Lima, 2004).

The catalytic domain of human RNase H1 shares strong sequence homology with *B. halodurans* RNase H (Wu, 1998). The structure of *B. halodurans* RNase H bound to the RNA/DNA heteroduplex indicates that the catalytic domain of the enzyme interacts differently with the nucleotides upstream of the scissile phosphate compared to the nucleotides downstream of the scissile phosphate (Fig. 8C) (Nowotany, 2005). For example, downstream of the scissile phosphate the enzyme interacts exclusively with the RNA strand contacting the phosphates and 2'-hydroxyls whereas, upstream of the scissile phosphate, the enzyme interacts with both the RNA strand and via the phosphate-binding pocket, the

Molecular Pharmacology Fast Forward. Published on October 6, 2006 as DOI: 10.1124/mol.106.025429
This article has not been copyedited and formatted. The final version may differ from this version.

phosphates and furanose rings of the DNA strand (Fig. 8C). In addition, the enzyme was shown to induce a bend in the DNA strand of the heteroduplex at the phosphate-binding pocket (Nowotany, 2005).

Our results are consistent with the observed enzyme induced bend in the heteroduplex (Nowotany, 2005). Both the conformationally flexible N-Me-T and TFI modifications positioned adjacent the phosphate binding pocket (positions 14 - 16) enhanced RNase H1 activity, although the influence of the N-Me-T modification was observed at a greater distance from the phosphate binding pocket than the TFI modification (Fig. 2, 5 and 8B). This is likely due to the fact that N-Me-T induces a greater perturbation in the structure of the substrate. Specifically, the TFI modification is predicted to Π-stack with the adjacent nucleotide to form a stable base-pair, whereas the methyl group at the N_3 of the N-Me-T modification is predicted to sterically interfere with the heterocycle of the opposing ribonucleotide prohibiting proper stacking with the adjacent residues (Kool, 2002; Saenger 1984). The predicted Π-stacking properties of the TFI modification also appear to play an important role in this structure as mismatched base-pairs adjacent the TFI modification, which presumably disrupt the Π-stacking interaction, resulted in slower cleavage rates (Fig. 6). Introducing conformational flexibility into the substrate appears to be most effective when the modifications are positioned adjacent the phosphate-binding pocket rather than at nucleotides interacting directly with the phosphate-binding pocket (Fig. 5 and 8D). Stable hydrogen bonds also appear to be required downstream the scissile

Molecular Pharmacology Fast Forward. Published on October 6, 2006 as DOI: 10.1124/mol.106.025429
This article has not been copyedited and formatted. The final version may differ from this version.

phosphate as slower cleavage rates were observed for the TFI substitutions at positions 7 and 8 (Fig. 5 and 8D).

Mismatch base-pairs appeared to induce a structure similar to the TFI modification. With the exception of the A/A mismatches, similar positional effects on the human RNase H1 activity were observed for both the mismatched base-pairs and TFI substitutions (Fig. 7). Surprisingly, the purine-purine A/A mismatch is isosteric with the TFI/A base-pair and therefore was predicted to have a similar effect on human RNase H1 activity (Fig. 1B). Unlike the TFI modification, mismatched base-pairs are capable of forming noncanonical hydrogen bonds with the opposing nucleotide (Leontis, 2002). These noncanonical hydrogen bonds have been shown to alter the local helical geometry of the duplex, which may account for the difference in cleavage activity between the A/A mismatch and the TFI modifications.

The human RNase H1 activities observed for the junction modifications appeared to be influenced by the MOE residues as these modifications exhibited significantly different effects on human RNase H1 activity when substituted into substrates containing unmodified DNA (Lima, 2004). For example, the southern biased 2'-S-Me-T modification had previously been shown not to support human RNase H1 activity as a single 2'-S-Me-T substitution in the oligodeoxyribonucleotide of the heteroduplex substrate significantly reduced the human RNase H1 cleavage rate (Lima, 2004). In contrast, the 2'-S-Me-T

Molecular Pharmacology Fast Forward. Published on October 6, 2006 as DOI: 10.1124/mol.106.025429
This article has not been copyedited and formatted. The final version may differ from this version.

positioned adjacent the MOE modification either enhanced (position 5) or had no effect (position 16) on human RNase H1 activity (Fig. 2). We posited that the reduction in human RNase H1 activity was due to the conformational transmission of the southern biased 2'-S-Me-T into the adjacent deoxyribonucleotides (Lima, 2004). In the case of the chimeric ASO, the northern biased MOE appears to counteract the conformational transmission of the southern biased 2'-S-Me-T. When positioned away from the MOE residues, however, the modified nucleotides exhibited similar effects on effects on human RNase H1 activity to those observed for a single modified nucleotide substitution in substrates containing unmodified DNA. For example, the reduction in human RNase H1 activity observed for the TFI modification positioned one and two nucleotides downstream of the scissile phosphate (positions 7 and 8) was also observed for a single 4-methylbenzimidazole substitution in an unmodified oligodeoxyribonucleotide (Lima, 2004). The 4-methylbenzimidazole deoxyribonucleotide is isosteric with TFI and does not form a hydrogen bond with the opposing ribonucleotide (Lima, 2004).

Chimeric ASOs containing 2'-alkoxy modified deoxyribonucleotides offer certain advantages including enhanced hybridization affinity and increased nuclease resistance leading to longer elimination half-lives in all species and reduced pro-inflammatory effects (for review see Crooke, 2001). Despite theses advantages, chimeric ASO exhibit significantly slower human RNase H1 cleavage rates compared to oligodeoxyribonucleotides (Fig. 2). The results presented here

Molecular Pharmacology Fast Forward. Published on October 6, 2006 as DOI: 10.1124/mol.106.025429
This article has not been copyedited and formatted. The final version may differ from this version.

demonstrate that the conformational transmission effects of the northern biased 2'-alkoxy nucleotides can be modulated with appropriately positioned modified nucleotides and suggest that the incorporation of these modifications into chimeric ASOs should improve the potency of the ASOs. For example, modifications that disrupt base stacking interactions or exhibit an eastern sugar conformation, (e.g., N-Me-T and 2'-ara-F-T) are preferred at the DNA/MOE junction adjacent the phosphate binding pocket (positions 14 - 16). On the other hand, modifications exhibiting conformational flexibility or the opposing southern sugar conformation, (e.g., TFI and 2'-S-Me-T) are preferred at the DNA/MOE junction adjacent the ribonucleotides downstream of the scissile phosphate (position 5). The TFI modification can be used to modulate the negative effects of the 2'-alkoxy residues both upstream and downstream of the scissile phosphate irrespective of the heterocycle of the opposing nucleotide. However, the TFI modification should be positioned adjacent stable base-pairs and not at sites that interact directly with the enzyme (Fig. 6 and 8D). Mismatch base-pairs can also be used to enhance the human RNase H1 activity of the chimeric ASOs, although predicting favorable noncanonical base-pair substitutions may prove more difficult than TFI substitutions (Fig. 7). Finally, given that the elimination half-lives and pro-inflammatory effects of chimeric ASO drugs are determined by the MOE residues, substitution of one or two MOE modifications at the junction should have only modest effects on the properties of these drugs.

References

Bondensgaard KM, Petersen SK, Singh VK, Kumar RR, Wengel J, and Jacobsen JP (2000). Structural studies of LNA:RNA duplexes by NMR: conformations and implications for RNase H activity. *Chem.-Eur. J.* **15**: 2687-2695

Crooke, ST (2001) in *Antisense Technology: Principles, Strategies and Applications* (Crooke, ST ed) pp 1-28, Marcel Dekker, Inc., New York

Denisov AY, Noronha AM, Wilds CJ, Trempe J-F, Po, RT, Gehring K, and Damha M (2001) Solution structure of an arabinonucleic acid (ANA)/RNA duplex in a chimeric hairpin: comparison with 2'-fluoro-ANA/RNA and DNA/RNA hybrids. *Nucleic Acids Res.* **29:** 4284-4293.

Fraser A, Wheeler P, Cook PD and Sanghvi YS (1993) Synthesis and conformational properties of 2'-deoxy-2'-methylthiopyrimidine and -purine nucleosides: Potential antisense applications. *J. Heterocycle Chem.* **30**:1277-1287.

Freier SM, and Altmann K-H (1997) The Ups and Downs of Nucleic Acid Duplex Stability: Structure-stability Studies on Chemically-modified DNA:RNA duplexes. *Nucleic Acids Res.* **25**: 4429-4443.

Kool ET (2002) Replacing the Nucleobases in DNA with Designer Molecules. *Acc. Chem. Res.* **35**: 936-943

Lai JS and Kool ET (2004) Selective pairing of polyfluorinated DNA bases. *J. Am. Chem. Soc.* **126**: 3040-3041

Leontis NB, Stombaugh J and Westhof E (2002) The non-Watson-Crick base pairs and their associated isostericity matrices. *Nucleic Acids Res.* **30**: 3497-3531

Li F, Sarkhel S, Wilds CJ, Wawrzak Z, Prakash TP and Manoharan M, Egli M (2006) 2'-Flouroarabino- and arabinonucleic acid show different conformations, resulting in deviating RNA affinities and processing of their heteroduplexes with RNA by RNase H. *Biochemistry* **45**: 4141-4152

Lima WF, Wu H and Crooke ST (2001) *in "Methods in Enzymology"* (Nicholson, A. W., Eds.) pp 430-9, Academic Press, San Diego, CA.

Lima WF, Wu H, Nichols J, Prakash TP, Ravikumar V and Crooke ST (2003) Human RNase H1 uses one tryptophan and two lysines to position the enzyme at the 3'-DNA/5'-RNA terminus of the heteroduplex substrate. *J. Biol. Chem.* **278**: 49860-49867.

Lima WF, Nichols JG, Wu H-J, Prakash TP, Migawa, MT, Wyrzykiewicz TK, Bhat B and Crooke ST (2004) Structural requirements at the catalytic site of the heteroduplex substrate for human RNase H1 catalysis. *J. Biol. Chem.* **279**: 36317-36326

Nishizaki T, Iwai S, Ohtsuka E and Nakamura H (1997) Solution structure of an RNA.2'-O-methylated RNA hybrid duplex containing an RNA.DNA hybrid segment at the center. *Biochemistry* **36**: 2577-2585

Nowotany N, Gaidamakov SA, Crouch RJ and Yang W (2005) Crystal structures of RNase H bound to an RNA/DNA hybrid: substrate specificity and metal-dependent catalysis. *Cell* **121**: 1005-1016

Saenger, W. (1984) *Principles of Nucleic Acid Structure*, Springer-Verlag, New York.

Sambrook J, Fritsch EF and Maniatis T (1989) in *Molecular Cloning. A Laboratory Manual,* 2nd sd., Cold Spring Harbor Laboratory Press, Cold Spring Harbor, NY

Scaringe SA, Wincott FE and Caruthers MH (1998)) RNA oligonucleotide synthesis via 5'-silyl-2'-orthoester chemistry. *J. Am. Chem. Soc.* **120**: 11820-1182.

Teplova M, Minasov G, Tereshko V, Inamati GB, Cook PD, Manoharan M and Egli M (1999) Crystal Structure and Improved Antisense Properties of 2'-*O*-(2'methoxyethyl)-RNA. *Nature* **6**: 535 – 539.

Wu H, Lima WF and Crooke ST (1998) Molecular cloning and expression of cDNA for human RNase H. *Antisense and Nucleic Acid Development* **8**: 53-61.

Wu H, Lima WF and Crooke ST (2001) Investigating the structure of human RNase H1 by site-directed mutagenesis. *J. Biol. Chem.* **276**: 23547-23553.

Wu H, Lima WF, Zhang H, Fan A, Sun H and Crooke ST (2004) Determination of the role of the human RNase H1 in the pharmacology of DNA-like antisense drugs. *J. Biol. Chem.* **279**: 17181-17189.

Molecular Pharmacology Fast Forward. Published on October 6, 2006 as DOI: 10.1124/mol.106.025429
This article has not been copyedited and formatted. The final version may differ from this version.

Figure legends

Figure 1: **Structure of the nucleotide modifications.** (A) Modified nucleotides containing conformationally biased sugars include: the southern biased 2'-methylthiothymidine (2'-S-Me-T), the northern biased locked nucleic acid (LNA) and the eastern biased 2'-ara-fluorothymidine (2'-ara-F-T). (B) Structures of the modifications designed to introduce conformational flexibility into the heteroduplex. These modifications include: 2'-methoxyethoxy-N-methylthymidine (N-Me-T) and tetrafluoroindole (TFI).

Figure 2: **Relative human RNase H1 initial cleavage rates and cleavage sites for chimeric heteroduplexes containing the various modified nucleotides at the DNA/MOE junctions.** Heteroduplex sequences are shown with the oligoribonucleotide oriented 5' to 3' (upper sequence) and chimeric ASO 3' to 5' (lower sequence). The modified nucleotides are shown in bold and the positions within the chimeric heteroduplexes in parentheses from the 5'-termini of the ASO.

Molecular Pharmacology Fast Forward. Published on October 6, 2006 as DOI: 10.1124/mol.106.025429
This article has not been copyedited and formatted. The final version may differ from this version.

The underlined sequences represent the positions of the MOE nucleotides. Lines indicate the position of the human RNase H1 cleavages on the heteroduplex substrate. The length of the lines indicates the intensity of the human RNase H1 cleavage band on the polyacrylamide gel for each respective site. Ratio V_0 represents the initial cleavage rates for the heteroduplex containing modified nucleotides at the MOE/DNA junction divided by the 5-10-5 chimeric substrate. The V_0 values are an average of three measurements with estimated errors of CV < 5%.

Figure 3: **Human RNase H1 cleavage patterns for chimeric heteroduplex sequences containing TFI deoxyribonucleotides at the MOE/ DNA junctions.** (A) Polyacrylamide gel analysis of the 5-10-5 heteroduplex substrate and 5-10-5 heteroduplex containing and the TFI deoxyribonucleotide at position 15; (B) the 4-11-5 heteroduplex substrate and 4-11-5 heteroduplex containing the TFI deoxyribonucleotide at position 5. The substrates were incubated in the absence

Molecular Pharmacology Fast Forward. Published on October 6, 2006 as DOI: 10.1124/mol.106.025429
This article has not been copyedited and formatted. The final version may differ from this version.

(Lanes 1) and presence of human RNase H1 for: 5 min. (Lanes 2); 10 min (Lanes 3); 15 min (Lanes 4); 30 min. (Lanes 5); and 60 min. (Lanes 6). The arrows indicate the position of the ribonucleotide opposing the TFI modification on the polyacrylamide gel. Heteroduplex sequences are shown with the oligoribonucleotide oriented 5' to 3' (upper sequence) and chimeric ASO 3' to 5' (lower sequence). The underlined sequences indicate the position of the MOE substitutions and **I** represent the position of the TFI deoxyribonucleotides. Lines indicate the position of the human RNase H1 cleavages on the heteroduplex substrate. The length of the lines indicates the intensity of the human RNase H1 cleavage band on the polyacrylamide gel for each respective site.

Figure 4: **Relative human RNase H1 initial cleavage rates for chimeric heteroduplexes containing point mutations at the ribonucleotides opposing the TFI deoxyribonucleotides.** Point mutations and TFI substitutions are shown in bold and the positions within the heteroduplex in parentheses from the 5'-

Molecular Pharmacology Fast Forward. Published on October 6, 2006 as DOI: 10.1124/mol.106.025429
This article has not been copyedited and formatted. The final version may differ from this version.

termini of the (ASO). Underlined sequences and Ratio V_0 are described in figure 2.

Figure 5: **Chimeric heteroduplexes containing TFI deoxyribonucleotides at various positions in the chimeric ASO.** TFI substitutions are shown in bold and the positions within the heteroduplex in parentheses from the 5'-termini of the (ASO). Underlined sequences and Ratio V_0 are described in figure 2.

Figure 6: **Relative human RNase H1 initial cleavage rates for chimeric heteroduplexes containing mismatch base-pairs adjacent to the TFI deoxyribonucleotides.** Point mutations and TFI substitutions are shown in bold and in parentheses within the heteroduplex from the 5'-termini of the (ASO). Underlined sequences and Ratio V_0 are as described in figure 2.

Figure 7: **Relative human RNase H1 initial cleavage rates for chimeric heteroduplexes containing mismatch base-pairs.** (A) Mismatched base-pairs

Molecular Pharmacology Fast Forward. Published on October 6, 2006 as DOI: 10.1124/mol.106.025429
This article has not been copyedited and formatted. The final version may differ from this version.

positioned at or near the 5'-MOE/3'-DNA junction (positions 4 – 7). (B) Mismatched base-pairs positioned at or near the 5'-DNA/3'-MOE junction (positions 13 – 16). Point mutations are shown in bold and in parentheses within the heteroduplex from the 5'-termini of the (ASO). Underlined sequences and Ratio V_0 are as described in figure 2.

Figure 8: **Model for the interaction of RNase H1 with the chimeric heteroduplex substrate.** (A) Conformational transmission of the MOE residues to the adjacent deoxyribonucleotides. The upper and lower heteroduplexes represent, respectively, the 5-10-5/RNA and 0-10-0/RNA substrates. Heteroduplexes are shown with the RNA strand oriented 5' to 3' and chimeric ASO 3' to 5'. The orange structures represent the C2-*endo* sugar conformation resulting in the A-form helical geometry and the blue structures represent the preferred H-form geometry. (B) The putative enzyme/nucleotide interactions for cleavage at ribonucleotides 12 (two upper heteroduplexes) and 10 (two lower heteroduplexes) of chimeric substrates containing cleavage rate enhancing

(yellow) and reducing (green) junction modifications. The arrow indicates the positions of the scissile phosphates. The orange and blue structures are as described in 8A. The brown and dark blue structures indicate the positions of the enzyme interactions with the substrate. (C) Schematic illustrating the positions of the RNA-binding (RNABD) and catalytic (CAT) domains of human RNase H1 on the chimeric heteroduplex. The Red and pink structures indicate the interactions between the enzyme and, respectively, the 2'-hydroxyls and heterocycle bases of the RNA strand. The dark green and light green structures indicate the interactions between the enzyme and, respectively, the deoxyribonucleotide sugars and heterocycle bases of the ASO. The black filled circles represent the enzyme/phosphate interactions. (D) Shifting the downstream TFI substitutions (5 – 8) toward the cleavage site at ribonucleotide 12 (upper heteroduplex) and the upstream TFI substitutions (16 – 13) toward the cleavage site at ribonucleotide 10 (lower heteroduplex). The arrows, red, pink, yellow and green structures are as described in 8C.

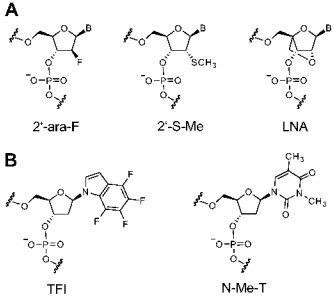

Figure_1AB

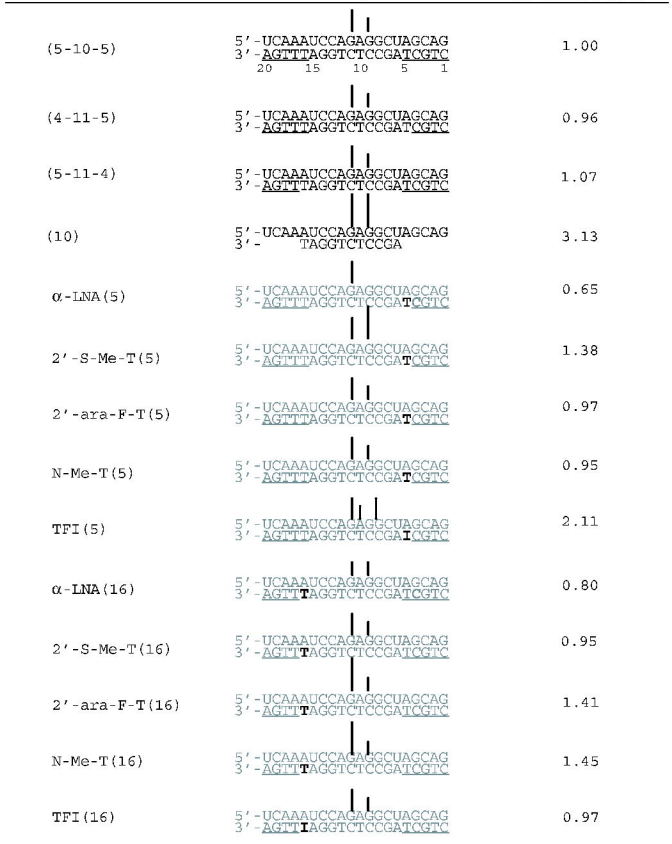
Modification
Heteroduplex
Ratio V0 (modified/5-10-5)
(5-10-5)
5′-UCAAAUCCAGAGGCUAGCAG
3′-AGTTTAGGTCTCCGATCGTC
20 15 10 5 1
1.00
(4-11-5)
5′-UCAAAUCCAGAGGCUAGCAG
3′-AGTTTAGGTCTCCGATCGTC
0.96
(5-11-4)
5′-UCAAAUCCAGAGGCUAGCAG
3′-AGTTTAGGTCTCCGATCGTC
1.07
(10)
5′-UCAAAUCCAGAGGCUAGCAG
3′- TAGGTCTCCGA
3.13
α-LNA(5)
5′-UCAAAUCCAGAGGCUAGCAG
3′-AGTTTAGGTCTCCGATCGTC
0.65
2′-S-Me-T(5)
5′-UCAAAUCCAGAGGCUAGCAG
3′-AGTTTAGGTCTCCGATCGTC
1.38
2′-ara-F-T(5)
5′-UCAAAUCCAGAGGCUAGCAG
3′-AGTTTAGGTCTCCGATCGTC
0.97
N-Me-T(5)
5′-UCAAAUCCAGAGGCUAGCAG
3′-AGTTTAGGTCTCCGATCGTC
0.95
TFI(5)
5′-UCAAAUCCAGAGGCUAGCAG
3′-AGTTTAGGTCTCCGAICGTC
2.11
α-LNA(16)
5′-UCAAAUCCAGAGGCUAGCAG
3′-AGTTTAGGTCTCCGATCGTC
0.80
2′-S-Me-T(16)
5′-UCAAAUCCAGAGGCUAGCAG
3′-AGTTTAGGTCTCCGATCGTC
0.95
2′-ara-F-T(16)
5′-UCAAAUCCAGAGGCUAGCAG
3′-AGTTTAGGTCTCCGATCGTC
1.41
N-Me-T(16)
5′-UCAAAUCCAGAGGCUAGCAG
3′-AGTTTAGGTCTCCGATCGTC
1.45
TFI(16)
5′-UCAAAUCCAGAGGCUAGCAG
3′-AGTTIAGGTCTCCGATCGTC
0.97

Figure_2

A

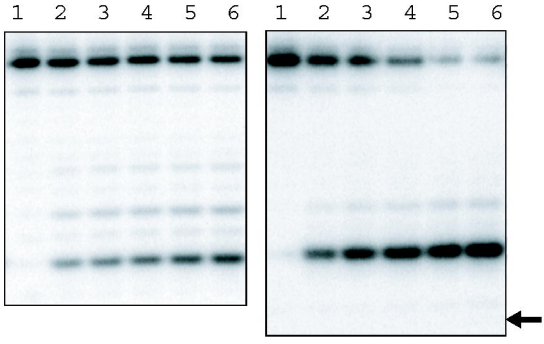
1 2 3 4 5 6
1 2 3 4 5 6
5-10-5
TFI

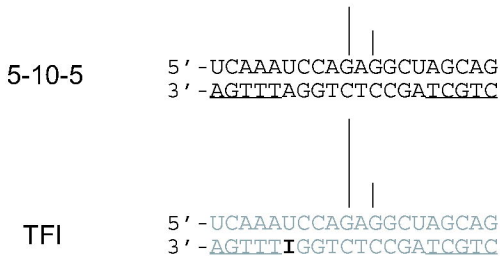
5-10-5
5′-UCAAAUCCAGAGGCUAGCAG
3′-AGTTTAGGTCTCCGATCGTC
TFI
5′-UCAAAUCCAGAGGCUAGCAG
3′-AGTTTIGGTCTCCGATCGTC

Figure_3A

B

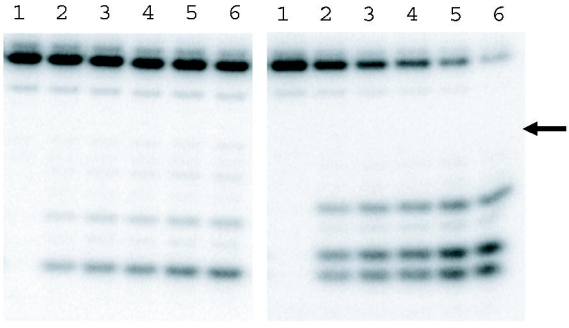
1 2 3 4 5 6
1 2 3 4 5 6
4-11-5
TFI


4-11-5
5′-UCAAAUCCAGAGGCUAGCAG
3′-AGTTTAGGTCTCCGATCGTC
TFI
5′-UCAAAUCCAGAGGCUAGCAG
3′-AGTTTAGGTCTCCGAICGTC

Figure _3B

Modification	Heteroduplex	Ratio V_0 (modified/5-10-5)
(5-10-5)	5′-UCAAAUCCAGAGGCUAGCAG 3′-AGTTTAGGTCTCCGATCGTC 20 15 10 5 1	1.00
TFI(5)	5′-UCAAAUCCAGAGGCUAGCAG 3′-AGTTTAGGTCTCCGA**I**CGTC	2.11
U/TFI(5)	5′-UCAAAUCCAGAGGCU**U**GCAG 3′-AGTTTAGGTCTCCGA**I**CGTC	1.88
TFI(15)	5′-UCAAAUCCAGAGGCUAGCAG 3′-AGTTT**I**GGTCTCCGATCGTC	1.93
A/TFI(15)	5′-UCAAA**A**CCAGAGGCUAGCAG 3′-AGTTT**I**GGTCTCCGATCGTC	1.74

Figure_4

Modification	Heteroduplex	Ratio V_0 (modified/5-10-5)
(5-10-5)	5′-UCAAAUCCAGAGGCUAGCAG 3′-AGTTTAGGTCTCCGATCGTC	1.00
TFI(4)	5′-UCAAAUCCAGAGGCUAGCAG 3′-AGTTTAGGTCTCCGATIGTC	1.06
TFI(5)	5′-UCAAAUCCAGAGGCUAGCAG 3′-AGTTTAGGTCTCCGAICGTC	2.11
TFI(6)	5′-UCAAAUCCAGAGGCUAGCAG 3′-AGTTTAGGTCTCCCITCGTC	1.10
TFI(7)	5′-UCAAAUCCAGAGGCUAGCAG 3′-AGTTTAGGTCTCCIATCGTC	0.66
TFI(8)	5′-UCAAAUCCAGAGGCUAGCAG 3′-AGTTTAGGTCTCIGATCGTC	0.78
TFI(17)	5′-UCAAAUCCAGAGGCUAGCAG 3′-AGTITAGGTCTCCGATCGTC	1.03
TFI(16)	5′-UCAAAUCCAGAGGCUAGCAG 3′-AGTTIAGGTCTCCGATCGTC	0.97
TFI(15)	5′-UCAAAUCCAGAGGCUAGCAG 3′-AGTTTIGGTCTCCGATCGTC	1.93
TFI(14)	5′-UCAAAUCCAGAGGCUAGCAG 3′-AGTTTAIGTCTCCGATCGTC	2.02
TFI(13)	5′-UCAAAUCCAGAGGCUAGCAG 3′-AGTTTAGITCTCCGATCGTC	1.09

Figure_5

Modification	Heteroduplex	Ratio V_0 (modified/5-10-5)
(5-10-5)	5′-UCAAAUCCAGAGGCUAGCAG 3′-AGTTTAGGTCTCCGATCGTC	1.00
TFI(5)	5′-UCAAAUCCAGAGGCUAGCAG 3′-AGTTTAGGTCTCCGAICGTC	2.11
G/A(4), TFI(5)	5′-UCAAAUCCAGAGGCUAGCAG 3′-AGTTTAGGTCTCCGAIAGTC	1.10
G/G(4), TFI(5)	5′-UCAAAUCCAGAGGCUAGCAG 3′-AGTTTAGGTCTCCGAIGGTC	0.94
TFI(7)	5′-UCAAAUCCAGAGGCUAGCAG 3′-AGTTTAGGTCTCCIATCGTC	0.66
U/G(6), TFI(7)	5′-UCAAAUCCAGAGGCUAGCAG 3′-AGTTTAGGTCTCCIGTCGTC	1.09
TFI(8)	5′-UCAAAUCCAGAGGCUAGCAG 3′-AGTTTAGGTCTCIGATCGTC	1.08
C/A(7), TFI(8)	5′-UCAAAUCCAGAGGCUAGCAG 3′-AGTTTAGGTCTCIAATCGTC	0.74
C/C(7), TFI(8)	5′-UCAAAUCCAGAGGCUAGCAG 3′-AGTTTAGGTCTCICATCGTC	0.60
TFI(15)	5′-UCAAAUCCAGAGGCUAGCAG 3′-AGTTTIGGTCTCCGATCGTC	1.93
C/T(14), TFI(15)	5′-UCAAAUCCAGAGGCUAGCAG 3′-AGTTTITGTCTCCGATCGTC	1.11
C/C(14), TFI(15)	5′-UCAAAUCCAGAGGCUAGCAG 3′-AGTTTICGTCTCCGATCGTC	1.10
TFI(14)	5′-UCAAAUCCAGAGGCUAGCAG 3′-AGTTTAIGTCTCCGATCGTC	2.02
C/T(13), TFI(14)	5′-UCAAAUCCAGAGGCUAGCAG 3′-AGTTTAITTCTCCGATCGTC	1.08
C/C(13), TFI(14)	5′-UCAAAUCCAGAGGCUAGCAG 3′-AGTTTAICTCTCCGATCGTC	0.88

Figure_6

A

Modification	Heteroduplex	Ratio V_0 (modified/5-10-5)
(5-10-5)	UCAAAUCCAGAGGCUAGCAG AGTTTAGGTCTCCGATCGTC	1.00
TFI(4)	UCAAAUCCAGAGGCUAGCAG AGTTTAGGTCTCCGATIGTC	1.06
G/A(4)	UCAAAUCCAGAGGCUAGCAG AGTTTAGGTCTCCGATAGTC	1.13
G/G(4)	UCAAAUCCAGAGGCUAGCAG AGTTTAGGTCTCCGATGGTC	1.08
TFI(5)	UCAAAUCCAGAGGCUAGCAG AGTTTAGGTCTCCGAICGTC	2.11
A/A(5)	UCAAAUCCAGAGGCUAGCAG AGTTTAGGTCTCCGAACGTC	0.72
U/A(5)	UCAAAUCCAGAGGCUUGCAG AGTTTAGGTCTCCGAACGTC	1.05
TFI(6)	UCAAAUCCAGAGGCUAGCAG AGTTTAGGTCTCCGITCGTC	1.10
U/G(6)	UCAAAUCCAGAGGCUAGCAG AGTTTAGGTCTCCGGTCGTC	0.94
TFI(7)	UCAAAUCCAGAGGCUAGCAG AGTTTAGGTCTCCIATCGTC	0.66
C/A(7)	UCAAAUCCAGAGGCUAGCAG AGTTTAGGTCTCCAATCGTC	0.70

Figure_7A

B

Modification	Heteroduplex	Ratio V_0 (modified/5-10-5)
(5-10-5)	UCAAAUCCAGAGGCUAGCAG AGTTTAGGTCTCCGATCGTC	1.00
TFI(16)	UCAAAUCCAGAGGCUAGCAG AGTT**I**AGGTCTCCGATCGTC	0.97
A/A(16)	UCAAAUCCAGAGGCUAGCAG AGTT**A**AGGTCTCCGATCGTC	0.66
TFI(15)	UCAAAUCCAGAGGCUAGCAG AGTTT**I**GGTCTCCGATCGTC	1.93
A/A(15)	UCAAA**A**CCAGAGGCUAGCAG AGTTT**A**GGTCTCCGATCGTC	1.49
A/U(15)	UCAAA**A**CCAGAGGCUAGCAG AGTTT**U**GGTCTCCGATCGTC	0.91
TFI(14)	UCAAAUCCAGAGGCUAGCAG AGTTTA**I**GTCTCCGATCGTC	2.02
C/T(14)	UCAAAUCCAGAGGCUAGCAG AGTTTA**T**GTCTCCGATCGTC	2.15
C/C(14)	UCAAAUCCAGAGGCUAGCAG AGTTTA**C**GTCTCCGATCGTC	1.90

Figure_7B

A

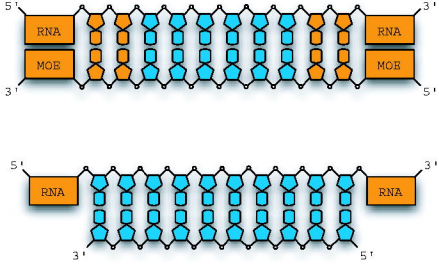

Figure_8A

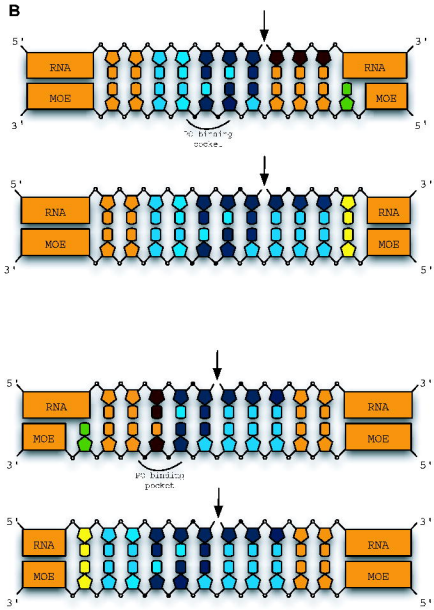

Figure_8B

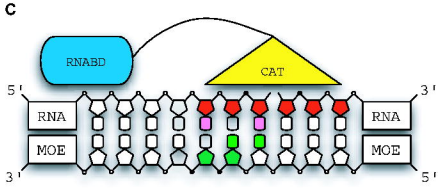

Figure_8C

D

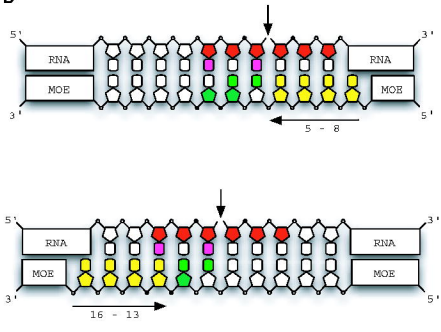

Figure_8D